Geminate Recombination versus Cage Escape in the Reductive Quenching of a Re(I) Carbonyl Complex on Mesoporous ZrO2

Oppelt, Kerstin ; Fernández-Terán, Ricardo ; Pfister, Rolf ; Hamm, Peter

Abstract: In the wider context of artificial photosynthesis, this work aims to explore the functionality and characteristics of rhenium tricarbonyl complexes as photosensitizers in heterogeneous water reduction systems. To that end, the reductive quenching of an excited ReICl(2,2 -bipyridine-4,4 -bisphosphonic acid)(CO)3 adsorbed on a redox-neutral scaffold by phenothiazine was observed by transient IR spectroscopy. From the spectroscopic and time response, the full reaction cycle could be elucidated, and the intrinsic lifetime of the excited Re complex, together with rates for reductive quenching, cage escape, as well as geminate recombination and secondary back electron transfer could be determined. Three different scenarios have been explored, which decrease the mobility of the reactants in the system in a stepwise manner: Starting from a reference system with all compounds in solution, first the Re complex was immobilized on the surface, and in a second step also the quencher. The overall reaction cycle for all reactants in solution is preserved as long as the quencher is in solution, with relatively minor changes of the rates of the individual reaction steps. The overall cage escape yield was found to be larger on the surface. As soon as the quencher is co-adsorbed alongside the Re-complex, however, the reaction cycle changes completely. Electron transfer occurred only from quencher molecules that sit next to an excited Re complex, and there is no possibility of cage escape. Varying the ratio of quencher molecules and Re-complexes, it is concluded that molecules do not cluster on the surface, and that excitation energy migration is not a very efficient process.

DOI: https://doi.org/10.1021/acs.jpcc.9b04950

Geminate Recombination versus Cage Escape in the Reductive Quenching of a Re(I) Carbonyl Complex on Mesoporous ZrO_2

Kerstin Oppelt*, Ricardo Fernández-Terán, Rolf Pfister and Peter Hamm

Department of Chemistry, University of Zurich. Winterthurerstrasse 190, Zurich, Switzerland.

ABSTRACT

In the wider context of artificial photosynthesis, this work aims to explore the functionality and characteristics of rhenium tricarbonyl complexes as photosensitizers in heterogeneous water reduction systems. To that end, the reductive quenching of an excited $Re^{I}Cl$(2,2′-bipyridine-4,4′-bisphosphonic acid)$(CO)_3$ adsorbed on a redox-neutral scaffold by phenothiazine was observed by transient IR spectroscopy. From the spectroscopic and time response, the full reaction cycle could be elucidated, and the intrinsic lifetime of the excited Re complex, together with rates for reductive quenching, cage escape, as well as geminate recombination and secondary back electron transfer could be determined. Three different scenarios have been explored, which decrease the mobility of the reactants in the system in a stepwise manner: Starting from a reference system with all compounds in solution, first the Re complex was immobilized on the surface, and in a second step also the quencher. The overall reaction cycle for all reactants in solution is preserved as long as the quencher is in solution, with relatively minor changes of the rates of the individual reaction steps. The overall cage escape yield was found to be larger on the surface. As soon as the quencher is co-adsorbed alongside the Re-complex, however, the reaction cycle changes completely. Electron transfer occurred only from quencher molecules that sit next to an excited Re complex, and there is no possibility of cage escape. Varying the ratio of quencher molecules and Re-complexes, it is concluded that molecules do not cluster on the surface, and that excitation energy migration is not a very efficient process.

INTRODUCTION

Artificial photochemical water splitting has led to the design of molecular systems that often consist of more than one component. In a typical scheme, the excited state of a photosensitizer (PS) is reductively quenched by an electron donor, and the quenched PS then transfers the electron to the actual hydrogen evolution catalyst.[1,2] Rhenium(I) tricarbonyls with bipyridyl ligands are widely used in multielectron processes such as carbon dioxide reduction, exploiting their photo- and electrochemical properties[3–7] for the formation of carbon monoxide or formate.[7–9] These complexes can also act as one-electron photosensitizers for photochemical water/proton reduction. The first reduction is usually reversible, as it is often located on the bipyridine ligand.[6,10–12] In combination with a cobalt-based water reduction catalyst[13–16] and a suitable electron donor reagent, photochemical water splitting has been observed in aqueous solution.[17–20] The initial quenching process of the excited photosensitizer with a sacrificial electron donor is the first key aspect of the overall photocycle the subsequent separation of the donor-acceptor contact pair from the common solvation shell (cage escape), to suppress back electron transfer by geminate recombination.

A heterogeneous system, where one or more of the reaction partners are surface-bound, allows for much higher concentrations of the various electron transfer partners than in solution, leading to shorter intermolecular distances, and therefore, to significantly faster charge transfer rates.[21] Since

reaction cycles in typical water-splitting systems are controlled kinetically, that might change the overall mechanism completely. For example, the initial step of reductive quenching remains diffusion-controlled if a sacrificial donor reagent in solution is used. In such a photocatalytic assembly, molecular diffusion to and from the surface has to be fast enough to reach the photosensitizer and/or photocatalyst in time.

While the mechanisms and energetics of the electron transfer processes in solution are well understood,[22–28] equivalent studies on surfaces are still comparably scarce. One example studied the diffusion-controlled quenching of a surface-bound ruthenium-based photosensitizer by photoluminescence,[29] but that spectroscopic method is blind to the subsequent processes; in particular to the cage escape yield and geminate recombination, which often limits the overall yield of an artificial water-splitting system. Here, by using transient IR spectroscopy, we can directly identify the redox state of the Re(I) complex on the surface also after the initial quenching event via the carbonyl stretch vibrations, which serve as spectroscopic markers for redox state of the Re center.[30,31]

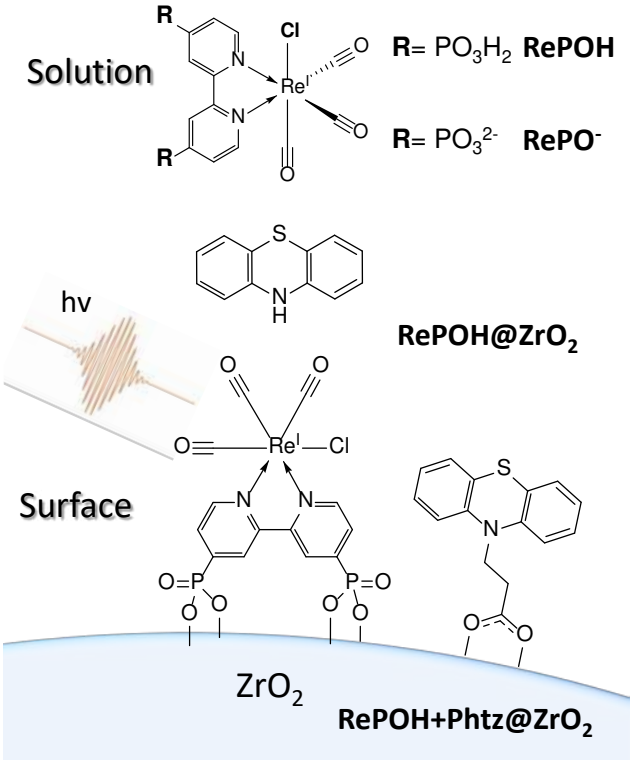

*Figure 1 Scheme of the investigated system of the rhenium carbonyl complex on the surface with the quencher in solution (**RePOH@ZrO₂**) and with the quencher co-adsorbed (**RePOH+Phtz@ZrO₂**). For comparison, a system with all compounds in solution has been considered as well with **RePOH** and **RePO⁻** as the electron acceptor.*

We chose [$Re^{I}Cl$(2,2′-bipyridine-4,4′-bisphosphonic acid)$(CO)_3$][32,33] adsorbed on ZrO_2 (**RePOH@ZrO₂**) for this purpose (Fig. 1). The bandgap and the band alignment of the ZrO_2 relative to the energy levels of the Re complex are such that the conduction band of the oxide is higher than the triplet excited state, and the valence band is lower than the depleted HOMO in the excited state. Indeed, it has been shown that ZrO_2 acts as an inert substrate, without electron injection from Re(I) carbonyl complexes.[34] As reductive quencher, we used phenothiazine derivatives, either in solution or surface bound via a carboxyl linker (phenothiazine-*N*-propionic acid). Phenothiazine derivatives have been shown to be

efficient quenchers for Re complexes with quenching constants (k_q) close to the diffusion limit (i.e., in the order of 10^9 M^{-1} s^{-1} in DMF).[22]

Three sets of experiments will be presented. In the first set, only the Re complex has been surface-bound, while the quencher was in EtOH solution. For comparison, we also considered in a second set of experiments a system with all compounds in solution; the quencher as well as fully protonated **RePOH** and fully deprotonated **RePO**$^-$ (Fig. 1). These two complexes have been selected as limiting cases, since the anchoring group is deprotonated at least once upon binding to the surface.[35] Comparing these two sets of experiments, we find that the kinetics of quenching and the subsequent charge transfer steps are affected only to a relatively minor extent by the surface. In a third set of experiments, the quencher has been co-adsorbed on the surface (**RePOH+Phtz@ZrO$_2$**, Figure 1), in which case the reaction cycle changes completely. That is, electron transfer occurs only from those quencher molecules that sit next to a Re complex, and there is no possibility of cage escape. By observing the kinetics as a function of the ratio between quencher and Re complex, we can estimate the morphology of molecules on these mixed surfaces and conclude that they do not cluster.

METHODS

The main method of investigation was transient IR spectroscopy. The spectrometer consists of two electronically-synchronized amplified Ti:sapphire lasers operating at 2.5 kHz.[36] This system allows pump–probe delay times from ≈10 ps to ≈40 μs, where the lower limit is a result of the jitter of the electronic synchronization. Pump pulses centered around 400 nm were generated from the first Ti:sapphire laser by frequency doubling. Tunable mid-IR probe pulses were obtained from the second Ti:sapphire laser in a home-built OPA.[37] The probe pulses were dispersed after the sample in a spectrograph and detected using a 2×64 pixel MCT detector, covering a 200 cm^{-1} spectral window with ca. 4 cm^{-1} resolution.

Significant degradation processes were observed during the course of a measurement once we exceeded a certain threshold of excitation energy. The pump laser energy used to ensure long term stability of the sample was kept below 200 nJ, and the pump pulses were focused to 330 μm (60 μJ/cm^{-2}). The chemical stability of the samples was further improved by using ethanol as a solvent,[38,39] and purging it with Ar. The sample was constantly moved during data acquisition using a home-built 2D raster scanner with magnetic linear motors. In addition to a noise-weighted averaging of the data, we found it beneficial to measure 10-20 batches of 100 shots per time delay, rejecting the batches with a noise level >1.3-1.5 times the average. This led to ca. 10 % of batches being discarded in an average scan, but was imperative for the signal quality. The sudden increases in the noise levels are attributed to surface imperfections.

Further description of the sample preparation, synthesis and characterization of the complexes by NMR, visible-light microscopy and SEM, as well as IR and UV/VIS spectra can be found in the supplementary information.

RESULTS

The FTIR spectrum of the surface-bound **RePOH@ZrO$_2$** (Fig. 2a) shows the three usual ν_{CO} bands a'', a'(1) and a'(2), which originate from the three -C≡O groups of the compound.[40,41] Their frequency positions are very similar to those of the corresponding bands in solution (see Fig. S1 of Supplementary Information), but the bands are somewhat broader.

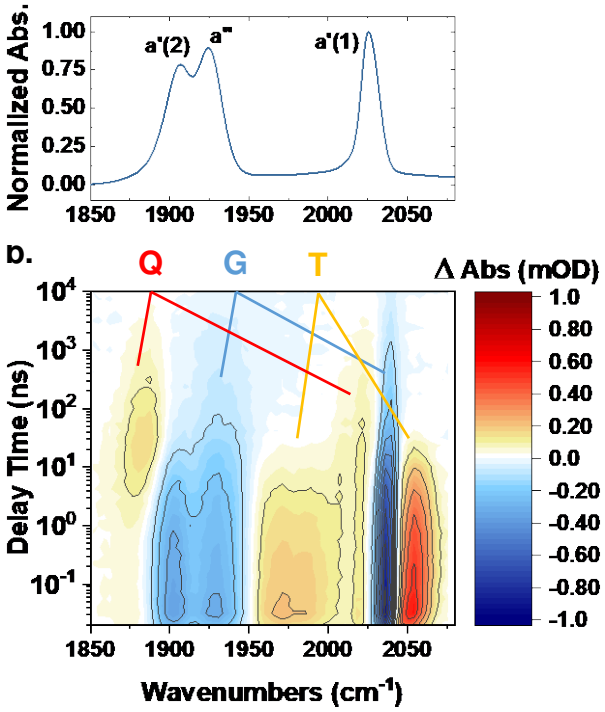

*Figure 2 (a) FTIR Spectrum of **RePOH@ZrO₂** with the EtOH background subtracted. (b) Transient IR spectrum of **RePOH@ZrO₂** with 100 mM phenothiazine in the EtOH solution.*

Fig. 2b exemplifies one transient IR experiment of **RePOH@ZrO₂** with 100 mM phenothiazine in EtOH solution. The optical transition leading to the metal-to-ligand-charge-transfer state (^{1}MLCT)[42] around 375-402 nm depending on the Re complex (see Fig. S2), is excited with short pulses around 400 nm, and the oxidation state of the Re-center is probed with mid-IR pulses centered at ≈1975 cm^{-1}. Immediately after excitation, the ground state **(G)** is depleted and the ν_{CO} bands appear as a negative (blue) bleach signal. Ultrafast intersystem crossing leads to the electronically excited triplet state **(T)**,[43] whose signatures can be seen as positive (red) signals at higher frequencies relative to the bleaches.[40,44] The MLCT corresponds to a formal oxidation of the Re center, lowering the amount of backbonding of the -C≡O groups, hence the frequency up-shift. The subsequent reductive quenching of the excited state by phenothiazine, in turn, results in a red shift of the ν_{CO} bands **(Q)**, and is clearly evidenced by the positive band appearing near 1875 cm^{-1} at ≈3-5 ns, remaining visible for delays up to 5-10 µs. The assignment of the reduced state compares well with the spectroelectrochemical results on a similar Re complex.[45] All raw data of the different sets of experiments that will be discussed below, equivalent to Fig. 2b, are shown in Figs. S3-S5.

The photocycle of the Rhenium complex presented here involves a reversible single electron transfer from the phenothiazine quencher. It has been observed that phenothiazine may irreversibly donate a second electron after deprotonation under certain conditions.[46,47] In our case, however, we observe the transfer of a single electron in a reversible manner, evidenced by the absence of permanent transient signals in Fig. 2b.

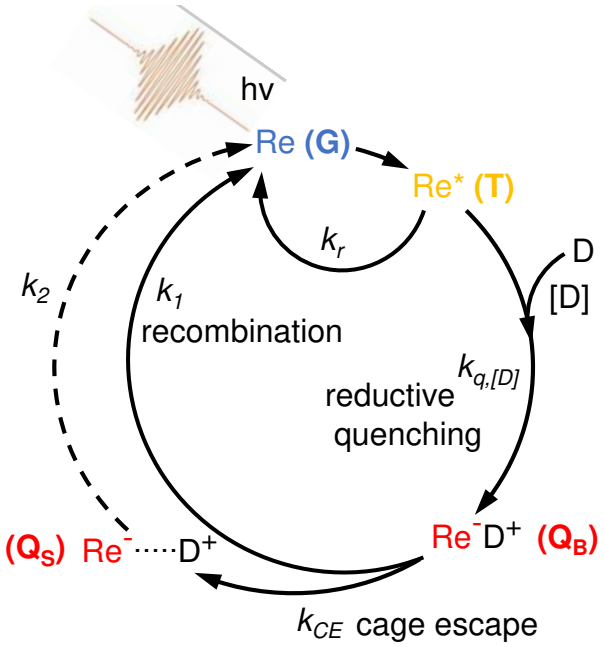

Figure 3 Reaction cycle (adapted from Ref. [48]) of the Re complex with an electron donating quencher molecule D. G is the ground state, T the triplet excited state, [D] is the concentration of D, Q_B the bound quenched state, Q_S the separated quenched state, k_r the rate of excitation relaxation, $k_{q,[D]}$ the concentration dependent quenching rate, k_{CE} is the cage escape rate, and k_1 and k_2 the back electron transfer rates (further details can be found in the text).

The transient IR data can be explained in terms of the reaction cycle shown in Fig. 3. To start with, there are two competing mechanisms that lead to relaxation of the electronically excited triplet state **(T)**. The first is the inherent relaxation of that state with a rate k_r that depopulates the excited state even without quencher (see Fig. S3a and S4a,e). In the presence of an electron donor, reductive quenching, taking place with a concentration-dependent rate $k_{q,[D]}$, represents the second deactivation pathway for the excited state, and hence shortens the lifetime (see Fig. S3b-d, S4b-d, 4f-h). Immediately after the quenching event, an ion pair Re^-Q^+ (**Q_B**) is formed within the same solvent cage. The two charged species might then escape from their solvent cage with the cage escape rate k_{CE} to form the separated quenched state (**Q_S**). **Q_B** and **Q_S** cannot be distinguished spectroscopically, rather, the observed transient signal corresponds to the sum **$Q = Q_B+Q_S$**. However, there are two recombination pathways on different timescales for **Q_B** and **Q_S**, and we will see later that both states can be separated by their different kinetic responses. That is, geminate recombination with rate k_1 involves direct electron back-transfer to the oxidized quencher before the separation of the Re^-Q^+ ion pair, while secondary back electron transfer with rate k_2 takes place after initial separation of the two species, which can re-encounter by diffusion.

In order to put the reaction cycle of Fig. 3 onto a more quantitative footing, we have adapted an analysis based on species-associated spectra.[49] To that end, the transient IR spectra were first globally fitted by linear combinations of Gaussian functions, keeping their center frequencies and line widths constant and allowing only their amplitudes to vary as a function of pump-probe delay time. These amplitudes are a measure of the relative population of the corresponding species, but also include their *per se* unknown absorption cross sections. The amplitudes were therefore re-normalized using the conservation of the overall population as a criterion (see Fig. S6 and SI for details). The results of this procedure are shown in Fig. 4 as symbols.

In a second step, the populations as a function of delay time were fit to the following kinetic model:

$$\partial_t \begin{pmatrix} [T] \\ [Q_b] \\ [Q_s] \\ [G] \end{pmatrix} = \begin{bmatrix} -k_{q,[D]} - k_r & 0 & 0 & 0 \\ k_{q,[D]} & -k_{CE} - k_1 & 0 & 0 \\ 0 & k_{CE} & -k_2 & 0 \\ k_r & k_1 & k_2 & 0 \end{bmatrix} \begin{pmatrix} [T] \\ [Q_b] \\ [Q_s] \\ [G] \end{pmatrix}, \quad (1)$$

which reflects the reaction cycle of Figure 3. The resulting fits are shown in Fig. 4 as solid lines. In the absence of quencher (Fig. 4, grey symbols), the decay of the triplet excited state **T** directly repopulates the ground state **G** with rate k_r, as evidence by the fact that the fit of the triplet excited state signal reveals the same time constant as the ground state recovery. Furthermore, while the exponential kinetics resulting from Eq. 1 fit the data for **RePOH** and **RePO**$^-$ in EtOH solution very well, the kinetics of **RePOH@ZrO$_2$** are better described by stretched exponentials. We attribute these stretched exponential kinetics to the heterogeneous environment on the surface, leading to a distribution of decay times. It is possible to fit the isolated decay of the triplet excited state with a stretched exponential function with τ=30 ns and a stretching factor of β=0.55; this fit is shown in Fig. 4c in light grey. With these numbers, an averaged lifetime ⟨τ⟩ can be calculated

$$\langle \tau \rangle = \frac{\tau}{\beta} \Gamma \left(\frac{1}{\beta} \right), \quad (2)$$

revealing ⟨τ⟩= 50 ns. However, in order to use a consistent rate model for the analysis of the full reaction cycle for solution and on the surface according to Eq. 1, we show the exponential fit also for **RePOH@ZrO$_2$** as grey solid line in Fig. 4, and consider the extracted time-constant (32 ns) an average decay time, which is in reasonable agreement with Eq. 2.

The lifetime of **RePOH@ZrO$_2$** lies in between those of the fully protonated **RePOH** (15 ns) and fully deprotonated **RePO**$^-$ complexes (60 ns) in EtOH solution (all rates are summarized in Table 1). Considering previous studies on the effect of bipyridine substituents on the excited-state lifetimes of similar complexes,[50] we suggest that these differences arise from the effect of the protonation state of the adsorbed complex.

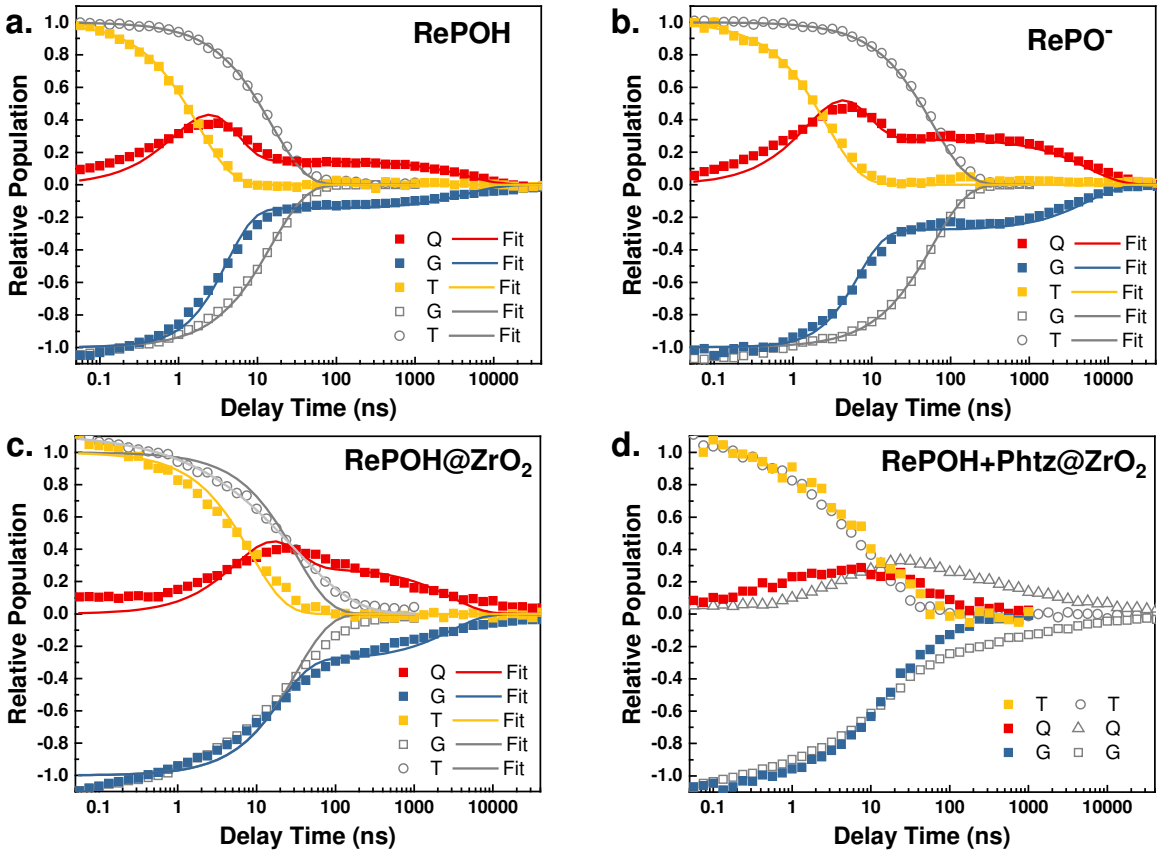

Figure 4 Relative populations (symbols) and kinetic model fit (lines) for (a) ***RePOH****, (b)* ***RePO⁻****, (c)* ***RePOH@ZrO₂*** *and (d)* ***RePOH+Phtz@ZrO₂****. In panels (a-c) 100 mM phenothiazine was added as quencher in solution and in panel (d) with quencher/Re ratio on the surface has been 3.7. In either case, blue depicts the ground state recovery, yellow the excited state decay and red the quenched state, and grey the excited state decay (circles) and ground state recovery (squares) in the absence of the quencher. In panel (c), the light-grey line shows a stretched exponential fit. In panel (d) the relative populations for* ***RePOH+Phtz@ZrO₂*** *(same color code) are compared to the signal of* ***RePOH@ZrO₂*** *with 100 mM quencher in solution (grey). The excitation intensity has been 60 μJ/cm², resulting in an excitation density of ≈1% in the case of* ***RePOH@ZrO₂****.*

Upon adding phenothiazine as a quencher, the triplet state decays faster (Fig. 4a-c, yellow), accompanied by the rise of a signal for the quenched state (red). The most remarkable feature in the kinetic traces of Fig. 4ab is the subsequent biphasic decay of the quenched species (red), which can only be reproduced in the kinetic model by explicitly distinguishing $\mathbf{Q_B}$ and $\mathbf{Q_S}$. Global fitting according to Eq. 1 reveals the rates k_1 and k_2 of their decays, as well as the cage escape rate k_{CE} (see Table 1). Compared to the reaction of similar Re complexes in water,[17,20] the kinetics of **RePOH** and **RePO⁻** upon quenching with phenothiazine are quite unusual, as geminate and secondary recombination processes give rise to such a distinct biphasic decay. Geminate recombination is well resolved since its rate k_1 is of the same order of magnitude as the cage escape rate k_{CE}. In that regard, it is important to note that the back electron transfer k_1 from phenothiazine is much faster than that of TEOA or quinones investigated before.[17,20]

For the surface-immobilized Re complex (**RePOH@ZrO₂**, Fig. 4c), the biphasic decay of the **Q** signal is not resolved very clearly, as it is blurred by the non-exponential kinetics due to the heterogeneous environment. Nevertheless, the overall timescale of the decay is very comparable to the results with the Re complex in solution (Fig. 4a,b), and we assume that both processes, geminate and secondary

recombination, occur in a similar fashion. Fitting the data to the same model of Eq. 1, which implicitly assumes exponential kinetics, reveals numbers for the average rates k_1, k_2 and k_{CE} on the surface (see Table 1), but we consider them less reliable than for the solution phase systems.

Another observation concerns the ground state bleach signal of **RePOH** and **RePO$^-$** in solution, which becomes shorter upon addition of the quencher (Fig. 4a,b blue versus grey). This speed-up can be explained by the fact that a significant fraction of the initially formed **Re$^-$Q$^+$** ion pair cannot separate efficiently and the system reaches the ground state largely by geminate recombination on a timescale that is significantly faster than the excited state relaxation k_r, i.e. $k_1 >> k_r$. On the surface, on the other hand, we find that addition of the same amount of quencher does not lead to faster recovery of the ground state. In other words, after the initial quenching event, the major fraction of **RePOH@ZrO$_2$** remains in the reduced state, since k_1 and k_r are of the same order of magnitude.

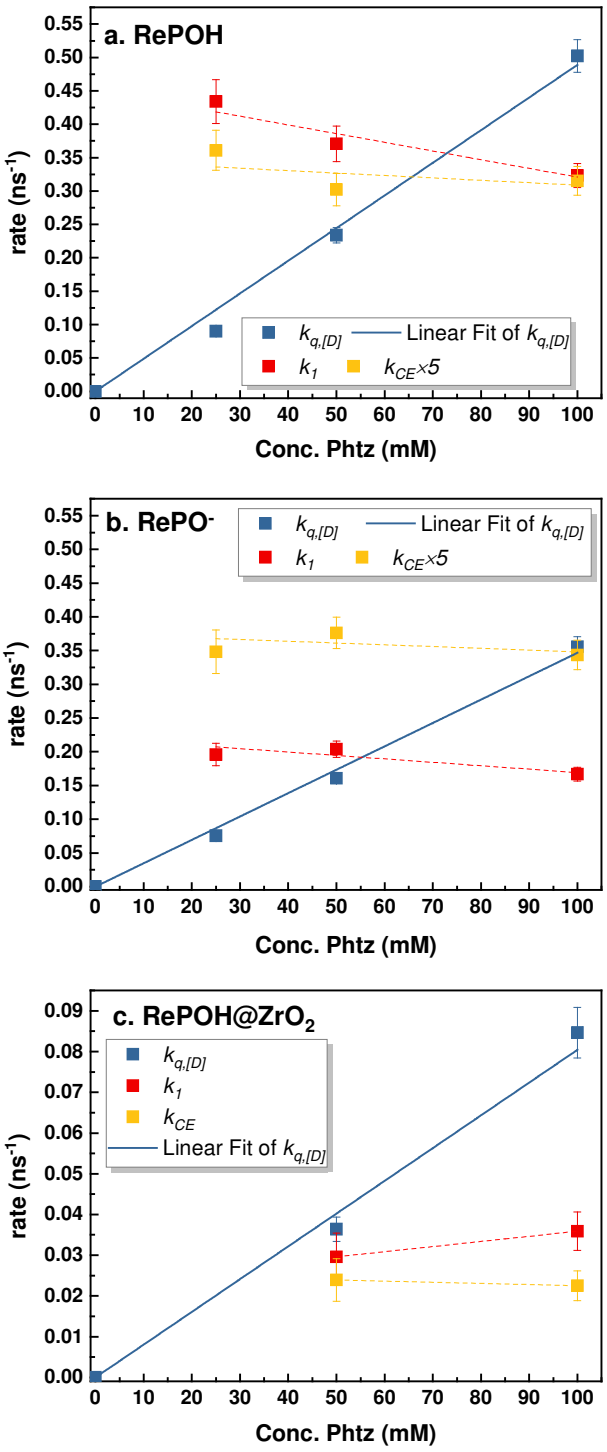

Figure 5 Rates $k_{q,[D]}$, k_1 and k_{CE} as a function of quencher concentration together with linear fits to guide the eyes. In the case of ***RePOH@ZrO₂*** *the excitation intensity has been 60 µJ/cm², resulting in an excitation density of ≈1%.*

The second-order quenching rate k_q can be obtained by analysis of the quenching rate $k_{q,[D]}$ as a function of the quencher concentration. To that end, the transient IR data were fit globally according to Eq. 1, fixing k_r to the value obtained from the experiments without quencher. As can be seen in Fig. 5 (blue squares), the quenching rate $k_{q,[D]}$ depends linearly on the quencher concentration, hence the

quenching constant k_q can be determined from the slope of a linear fit to $k_{q,[D]}$ (Fig. 5, blue line). In contrast, k_1 does not depend on the quencher concentration (Fig. 5, red). This constitutes the main evidence suggesting that k_1 represents the primary geminate recombination event, which is an effectively unimolecular process with respect to the kinetics. The same applies for the cage escape rate k_{CE} (Fig. 5, yellow).

The recombination rate k_2 should correspond to a bimolecular process as well, but the relevant concentrations are those of the reduced Re complexes and the oxidized quencher, not the initial concentration of the quencher. However, a model treating k_2 as a pseudo-first-order reaction rate (Eq. 1) reproduced our solution data slightly better than a model calculating k_2 as a bimolecular rate (a comparison of the fits assuming pseudo-first-order vs second order kinetics can be found in the SI, see Fig. S7). This can be attributed to an excess of oxidized D^+ already present in the solution. At the excitation density used, the transient concentration of the reduced Re complex (a few µM) is by orders of magnitudes lower than that of the quencher (100 mM), hence, even minor impurities, e.g., by trace amounts of oxygen, will render the D^+ concentration larger than that of reduced Re complex. . In light of this discussion, we did not attempt to determine the second–order recombination rate k_2.

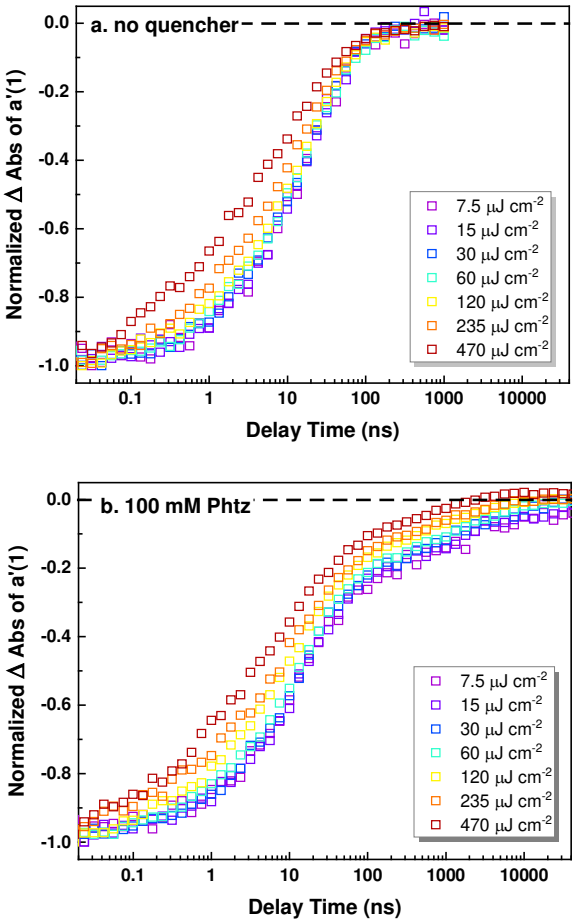

*Figure 6. Normalized transient IR ground state bleach traces at 2075 cm^{-1} as a function of the excitation intensity for **RePOH@ZrO₂** (a) without quencher and (b) with 100 mM phenothiazine in EtOH.*

We also varied the excitation laser energy. It turned out that the excitation energy strongly influenced the relaxation rate k_r (Fig. 6a), revealing a faster and more non-exponential decay process at higher laser power due to bimolecular excited state quenching, presumably due to triplet-triplet-annihilation.[51] This influenced all following processes such that there was almost no formation of reduced rhenium at higher pump power, as seen by the lower amplitude of the long-lived signal beyond 100 ns in Fig. 6b. The values reported in Table 1 are for a pump intensity of 60 µJ/cm^2. At this pump intensity, the excitation density is ≈1%, as estimated from the size of the transient bleach signal of the a'(1) mode (1.2 mOD, see Fig. S8) relative to the absorbance of that mode in the stationary spectrum (120 mOD). It is important to keep in mind that this estimate ignores a difficult to determine anisotropy factor, as the absorbance in a stationary spectrum averages over all orientations in the sample, while the polarization of the pump-pulse preselects a certain sub-ensemble in a transient spectrum. In any case, an excitation density in the range of ≈1% is low enough so that bimolecular excited state quenching does not yet play a significant role (Fig. 6, cyan data). Beyond a pump intensity of 120 µJ/cm^2 (yellow data in Fig. 6), bimolecular excited state quenching becomes visible and starts to dominate at 470 µJ/cm^2 (dark-red data in Fig. 6).

Assuming a closest ball packing with typically 6 nearest neighbors on the surface, the latter corresponds to a probability of ≈50% that a given excited Re complex has another excited Re complex as nearest neighbor (including the same uncertainty regarding the anisotropy factor mentioned above). This very rough estimate is consistent with the notion that triplet-triplet-annihilation is short-ranged as the underlying Dexter energy transfer mechanism requires an orbital overlap of donor and acceptor molecules. We therefore conclude that triplet-triplet annihilation occurs predominantly between nearest neighbors. Since the arrangement of Re complexes on the surface presumably is disordered to a certain extent, there will be a distribution of intermolecular distances, which together with the strong distance dependence of triplet-triplet annihilation explains in part the observed non-exponential kinetics.

*Table 1 Summary of rate constants and cage escape yields obtained from the kinetic analysis of the data. All rates were determined for an excitation intensity of 60 µJ/cm^2, resulting in an excitation density of ≈1% in the case of **RePOH@ZrO$_2$**.*

	k_r (10^6 s^{-1})	k_q (10^6 s^{-1}M^{-1})	k_1 (10^6 s^{-1})	k_{CE} (10^6 s^{-1})	k_2* (10^6 s^{-1})	η_{CE}** (%)
RePOH (in EtOH)	66	4900	380	65	0.16	15
RePO$^-$ (in EtOH)	17	3500	190	71	0.21	26
RePOH@ZrO$_2$	31	800	22	16	0.21	42

* k_2 was treated as quasi-first order kinetics, accounting for the fact that an excess of oxidized quencher exists due to trace amounts of impurities. The extracted value for k_2 may therefore depend on sample preparation. ** The cage escape yield[52] was calculated from: $\eta_{CE} = k_{CE}/(k_1 + k_{CE})$;

We now turn to the experiments with the quencher co-immobilized on the surface **(RePOH+Phtz@ZrO$_2$)**, starting with a quencher/Re-ratio of 3.7 in Fig. 4d (the ratio has been determined from the intensities of IR marker modes of both molecules, see Fig. S9). The first observation is an accelerated build-up and decay of the quenched species, in comparison to the result with the quencher in solution (see Fig. 4d, red vs grey). That acceleration can be attributed to the fact

that the quenching is no longer diffusion-controlled in this case. Instead, the quencher molecules are already sitting next to the Re complex at a distance that is dictated by the morphology of the molecules on the surface. The very non-exponential character of the build-up is again attributed to a relatively wide distribution of inter-molecular distances and the fact that electron transfer has a very strong distance dependence. On the other hand, given the very high effective concentration on a surface, the only rather modest acceleration of the buildup might seem surprising. However, the timescale is about the same as that observed for the intramolecular electron transfer between a similar Re complex and a covalently linked phenothiazine moiety in a supramolecular construct.[23,53,54] Depending on substituents, electron transfer occurred with rates between $2 \cdot 10^8$ - $5 \cdot 10^9$ s^{-1}, which is relatively slow despite the quite short donor-acceptor distances; an effect that has been attributed to the fact that electron transfer operates in the Marcus inverted regime.[23,53,54]

Regarding the back-electron transfer, there is no possibility for a cage escape when the quencher is immobilized on the surface, and geminate recombination dominates. Indeed, the timescale of back-electron transfer for the sample with the quencher co-adsorbed on the surface (a few 10 ns; we did not attempt a fit of the data due to the very non-exponential character of the kinetics) is in the same order of magnitude as k_1 for the samples with the quencher in solution ($22 \cdot 10^6$ s^{-1}, see Table 1). The consistency of these numbers reconfirms our earlier conclusion that cage escape does indeed take place in the latter case.

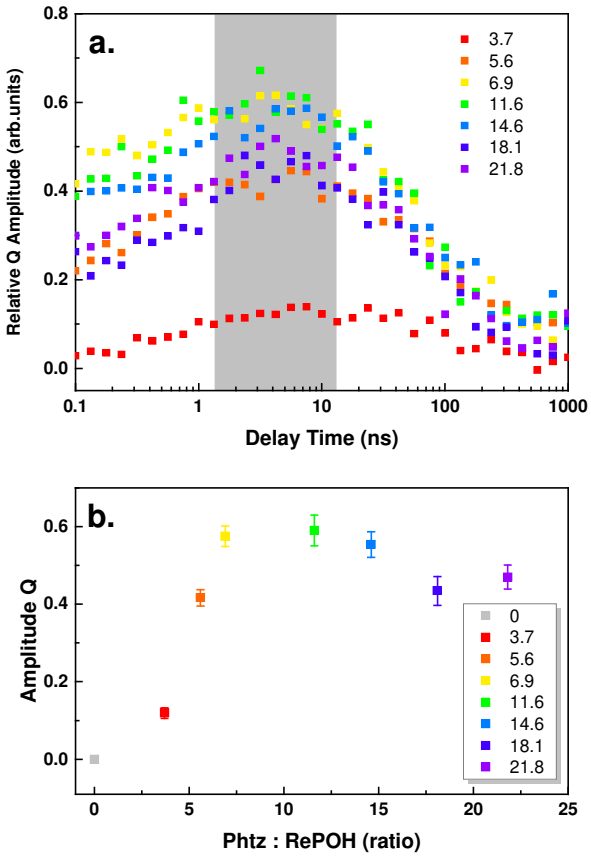

Figure 7 (a) Time evolution of Q for different ratios of phenothiazine-N-propionic acid on ZrO_2. (b) Relative amplitude for the reduced rhenium (i.e. the yield of Q) with increasing quencher ratio on the surface as represented by the average over the values in the grayed area in panel (a), i.e., averaged from 1.3 ns to 13 ns.

Fig. 7a shows the quenched Re signal with the quencher:Re ratio varied between 3.7 and 22 and Fig. 7b shows the peak of that signal (averaged from 1.3 ns to 13 ns) as a function of quencher:Re ratio. In the investigated range, the quencher is always in excess, and the number of quencher molecules *per se* should not be the limiting factor. Nevertheless, the amount of quenched Re complexes increases linearly for ratios up to ≈6 and saturates only beyond. Two conclusions can be drawn from this observation. Firstly, there is only next neighbor quenching. Just like for triplet-triplet annihilation, electron transfer is short-ranged as it relies on orbital overlap between donor and acceptor molecules. For quencher:Re ratios smaller than the threshold of 6, the likelihood of a quencher molecule sitting next to a Re complex increases linearly, assuming a closest ball packing on the surface (Fig. 8a). Beyond that, in the dilute limit with a large excess of quencher molecules, each Re complex is surrounded by typically 6 quencher molecules already (Fig. 8b), and increasing the quencher concentration will no longer enhance quenching. Secondly, the Re complexes do not cluster on the surface, but rather are randomly distributed at any quencher concentration. If they would cluster, Re complexes inside such a cluster would not have a quencher as nearest neighbor (Fig. 8c), hence quenching would be very inefficient and the dependence on quencher concentration would be expected to be weak.

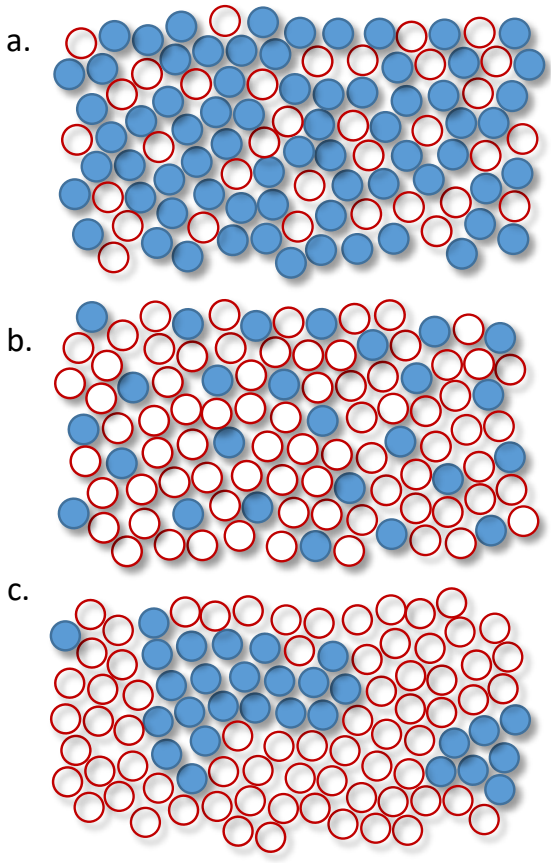

Figure 8. Sketch of possible scenarios for the surface morphology of ***RePOH+Phtz@ZrO₂*** *with (a) a small quencher:Re ratio, (b) a large quencher/Re-ratio and (c) a quencher/Re-ratio ratio of roughly 1, but with the molecules clustering on the surface. The Re complexes are shown as blue circles, the quencher molecules as red circles.*

DISCUSSION AND CONCLUSION

In this work, we investigated the quenching and recombination dynamics of a surface bound metal catalyst on a redox neutral scaffold using **RePOH** and phenothiazine as reactants. The phosphonate substituents on the bipyridyl ligand used to bind the rhenium complex to the surface decrease the excited state lifetime of the Re complex by factors of around 10 compared to similar complexes without such substituents.[18,19] A photochemical system using these short-lived complexes either in solution or on a surface needs an efficient quenching process to obtain sufficient reduced rhenium to drive a catalytic cascade. By exploiting the similarities of quenching and electron back transfer steps between a homogeneous system in solution and a system in which the Re complex is immobilized on the surface, we could derive the quenching and electron back transfer rates for the surface bound reactant(s).

The overall reaction cycle is not affected dramatically on the surface, despite the fact that the substrate is a mesoporous film from 20 nm ZrO_2 nanoparticles that is about 2 μm thick. Apparently, due to the large size of the pores in relation to the size of the quencher molecule (Fig. S10), the quencher molecules can diffuse relatively freely inside the mesoporous network. Small modifications can however be observed. For example, the first electron transfer process in the reaction cycle (i.e., the quenching rate k_q) slows down by a factor 4-6 on the surface (see Table 1). If we assume a flat surface, only one side of a molecule immobilized on the surface is accessible for a quencher molecule, explaining a twofold reduction of the quenching rate. Another factor two is obtained from the fact that only one of the reaction partners is freely diffusing in this case, and that a diffusion-controlled reaction rate scales linearly with the sum of the diffusion coefficients of the two components.[55]

Looking at the quenching event from a more atomistic point of view, the electronic excitation of the Re complex involves a formal reduction of the bipyridine ligand, leading to a $[Re^{II}(CO)_3(bpy^{\bullet-})Cl]$ species.[45] In solution, this molecule is able to rotate. On the surface, this rotation is hindered, and the molecules adsorb with well-defined orientations.[56,57] The degrees of freedom to obtain an optimal conformation for charge transfer that are therefore quite restricted on the surface, leading to a slower forward electron transfer rate.

It is interesting to note that the cage escape rate k_{CE} is slowed down by the same factor 4-6 as the quenching rate k_q. The cage escape rate reflects exclusively a diffusive process, without masking it with an additional electron transfer rate. However, since the quenching rate k_q is diffusion-controlled, both exhibit the same geometrical effects. The recombination rate k_1, in contrast, is slowed down by an even larger factor ≈10. This somewhat larger effect might be explained by the fact that the charge is transferred closer to the surface by the initial ultrafast MLCT in the Re-complex, and hence is spatially separated from the oxidized quencher molecules.

The amount of long-lived reduced Re complex (**Q**) is also determined by the cage escape yield η_{CE} (see Table 1). The cage escape yield describes the fraction of reduced Re-complexes that survive geminate recombination relative to those that are initially reduced. Those reduced Re complexes are long-lived and hence could potentially be used for further reactions such as transferring an electron to a catalyst. Somewhat counterintuitively, **RePOH@ZrO_2** performs better with regard to the cage escape yield, despite the fact that the quenching rate is slowed down. The cage escape yield is given by $\eta_{CE} = k_{CE}/(k_1 + k_{CE})$, hence it is the larger effect of the surface on k_1 in comparison to k_{CE}, which renders the cage escape yield larger on the surface.

If both the Re complex and the quencher are immobilized on the surface, as for **RePOH+Phtz@ZrO_2**, forward and backward electron transfer become slightly faster and reach values that are similar to those observed for intramolecular electron transfer reactions in supramolecular complexes with a covalently linked quencher moiety. For this electron transfer couple the electron transfer rates are not particularly fast, as it is thought to perform in the Marcus inverted region.[23,54] From the dependence

of the maximum amount of reduced Re complex on the quencher:Re ratio (Fig. 7), which levels off at ≈6, we concluded that quenching happens only between next neighbors and that the molecules do not cluster on the surface.

The power dependence of the excited state lifetime shown in Fig. 6 evidences that excited molecules sitting next to each other can exchange energy, presumably via triplet-triplet annihilation. Triplet-triplet annihilation is based on Dexter energy transfer and as such is short-ranged. One may assume that if triplet-triplet annihilation is possible, excitation energy migration via Dexter energy transfer should be possible as well.[58,59] While we cannot exclude some degree of excitation energy migration, the results of Fig. 7 speak against the fact that it is a dominating process. That is, if excitation migration would be very fast compared to the timescale of quenching, the data in Fig. 7 would in essence not be dependent on the quencher/Re-ratio, since an excitation then would always "find" a quencher molecule.

To conclude, we investigated the mechanisms and timescales of energy and electron transfer processes between surface-immobilized molecules, which are promising candidates for an electron shuttle and a photosensitizer in a complete photocatalytic system for water splitting. By a subtle effect, the cage escape yield can in fact be larger on the surface, and consequently, a larger amount of reduced Re-complexes will be available for the subsequent electron transfer step to a water reduction catalyst, which will the next step in this research. On the other hand, non-productive quenching of the excited state of the Re complexes becomes an issue due to the very large effective concentrations on the surface. As such, the present work provides two main design criteria for the development of a functioning heterogeneous system for artificial photosynthesis.

SUPPORTING INFORMATION:

Description of the sample preparation, synthesis and characterization of the complexes by NMR, visible-light microscopy and SEM, IR and UV/VIS spectra, a complete set of the tr-IR raw data, and a thorough description of the data analysis.

AUTHOR INFORMATION:

E-mail: kerstin.oppelt@chem.uzh.ch, peter.hamm@chem.uzh.ch

ACKNOWLEDGEMENTS:

Imaging was performed with support of the Center for Microscopy and Image Analysis, University of Zurich. Jan Helbing, Benjamin Probst, Roger Alberto and Laurent Sévery are gratefully acknowledged for helpful discussions. We especially acknowledge the contributions from Martin Haller and Roland Zehnder from the University of Zurich machine shop for the construction of the 2D raster scanner. We also thank Prof. Serdar N. Sariciftci and Christoph Ulbricht from LIOS at the Johannes Kepler University of Linz for the possibility to use the Nikon Eclipse LV100ND light microscope. We gratefully acknowledge financial support by the Swiss National Science Foundation (Grant CRSII2_160801/1) and the University Research Priority Program (URPP) for Solar Light to Chemical Energy Conversion (LightChEC) of the University of Zurich.

REFERENCES:

(1) Kalyanasundaram, K.; Kiwi, J.; Grätzel, M. Hydrogen Evolution from Water by Visible Light, a Homogeneous Three Component Test System for Redox Catalysis. *Helv. Chim. Acta* **1978**, *61* (7), 2720–2730. https://doi.org/10.1002/hlca.19780610740.

(2) Du, P.; Schneider, J.; Jarosz, P.; Eisenberg, R. Photocatalytic Generation of Hydrogen from Water Using a Platinum(II) Terpyridyl Acetylide Chromophore. *J. Am. Chem. Soc.* **2006**, *128* (24), 7726–7727. https://doi.org/10.1021/ja0610683.

(3) Morimoto, T.; Nakajima, T.; Sawa, S.; Nakanishi, R.; Imori, D.; Ishitani, O. CO 2 Capture by a Rhenium(I) Complex with the Aid of Triethanolamine. *J. Am. Chem. Soc.* **2013**, *135* (45), 16825–16828. https://doi.org/10.1021/ja409271s.

(4) Hawecker, J.; Lehn, J.-M.; Ziessel, R. Electrocatalytic Reduction of Carbon Dioxide Mediated by Re(Bipy)(CO)3Cl (Bipy = 2,2'-Bipyridine). *J. Chem. Soc. Chem. Commun.* **1984**, *6* (6), 328–330. https://doi.org/10.1039/c39840000328.

(5) Juris, A.; Campagna, S.; Bidd, I.; Lehn, J. M.; Ziessel, R. Synthesis and Photophysical and Electrochemical Properties of New Halotricarbonyl(Polypyridine)Rhenium(I) Complexes. *Inorg. Chem.* **1988**, *27* (22), 4007–4011. https://doi.org/10.1021/ic00295a022.

(6) Smieja, J. M.; Kubiak, C. P. Re(Bipy-TBu)(CO)3Cl-Improved Catalytic Activity for Reduction of Carbon Dioxide: IR-Spectroelectrochemical and Mechanistic Studies. *Inorg. Chem.* **2010**, *49* (20), 9283–9289. https://doi.org/10.1021/ic1008363.

(7) Hawecker, J.; Lehn, J.-M.; Ziessel, R. Photochemical and Electrochemical Reduction of Carbon Dioxide to Carbon Monoxide Mediated by (2,2?-Bipyridine)Tricarbonylchlororhenium(I) and Related Complexes as Homogeneous Catalysts. *Helv. Chim. Acta* **1986**, *69* (8), 1990–2012. https://doi.org/10.1002/hlca.19860690824.

(8) Abdellah, M.; El-Zohry, A. M.; Antila, L. J.; Windle, C. D.; Reisner, E.; Hammarström, L. Time-Resolved IR Spectroscopy Reveals a Mechanism with TiO 2 as a Reversible Electron Acceptor in a TiO 2 –Re Catalyst System for CO 2 Photoreduction. *J. Am. Chem. Soc.* **2017**, *139* (3), 1226–1232. https://doi.org/10.1021/jacs.6b11308.

(9) Windle, C. D.; Pastor, E.; Reynal, A.; Whitwood, A. C.; Vaynzof, Y.; Durrant, J. R.; Perutz, R. N.; Reisner, E. Improving the Photocatalytic Reduction of CO_2 to CO through Immobilisation of a Molecular Re Catalyst on TiO_2. *Chem. - A Eur. J.* **2015**, *21* (9), 3746–3754. https://doi.org/10.1002/chem.201405041.

(10) Sampson, M. D.; Froehlich, J. D.; Smieja, J. M.; Benson, E. E.; Sharp, I. D.; Kubiak, C. P. Direct Observation of the Reduction of Carbon Dioxide by Rhenium Bipyridine Catalysts. *Energy Environ. Sci.* **2013**, *6* (12), 3748. https://doi.org/10.1039/c3ee42186d.

(11) Machan, C. W.; Sampson, M. D.; Chabolla, S. A.; Dang, T.; Kubiak, C. P. Developing a Mechanistic Understanding of Molecular Electrocatalysts for CO2 Reduction Using Infrared Spectroelectrochemistry. *Organometallics* **2014**, *33* (18), 4550–4559. https://doi.org/10.1021/om500044a.

(12) Benson, E. E.; Kubiak, C. P. Structural Investigations into the Deactivation Pathway of the CO2 Reduction Electrocatalyst Re(Bpy)(CO)3Cl. *Chem. Commun. (Camb).* **2012**, *48* (59), 7374–7376. https://doi.org/10.1039/c2cc32617e.

(13) Eckenhoff, W. W. T.; McNamara, W. R. W.; Du, P.; Eisenberg, R. Cobalt Complexes as Artificial Hydrogenases for the Reductive Side of Water Splitting. *Biochim. Biophys. Acta - Bioenerg.* **2013**, *1827* (8–9), 958–973. https://doi.org/http://dx.doi.org/10.1016/j.bbabio.2013.05.003.

(14) McCormick, T. M.; Han, Z.; Weinberg, D. J.; Brennessel, W. W.; Holland, P. L.; Eisenberg, R. Impact of Ligand Exchange in Hydrogen Production from Cobaloxime-Containing Photocatalytic Systems. *Inorg. Chem.* **2011**, *50* (21), 10660–10666. https://doi.org/10.1021/ic2010166.

(15) Lazarides, T.; McCormick, T.; Du, P.; Luo, G.; Lindley, B.; Eisenberg, R. Making Hydrogen from Water Using a Homogeneous System without Noble Metals. *J. Am. Chem. Soc.* **2009**, *131* (26), 9192–9194. https://doi.org/10.1021/ja903044n.

(16) Hollmann, D.; Gärtner, F.; Ludwig, R.; Barsch, E.; Junge, H.; Blug, M.; Hoch, S.; Beller, M.; Brückner, A. Insights into the Mechanism of Photocatalytic Water Reduction by DFT-Supported in Situ EPR/Raman Spectroscopy. *Angew. Chemie Int. Ed.* **2011**, *50* (43), 10246–10250. https://doi.org/10.1002/anie.201103710.

(17) Probst, B.; Rodenberg, A.; Guttentag, M.; Hamm, P.; Alberto, R. A Highly Stable Rhenium-Cobalt System for Photocatalytic H(2) Production: Unraveling the Performance-Limiting Steps. *Inorg. Chem.* **2010**, *49* (14), 6453–6460. https://doi.org/10.1021/ic100036v.

(18) Probst, B.; Guttentag, M.; Rodenberg, A.; Hamm, P.; Alberto, R. Photocatalytic H2 Production from Water with Rhenium and Cobalt Complexes. *Inorg. Chem.* **2011**, *50* (8), 3404–3412. https://doi.org/10.1021/ic102317u.

(19) Guttentag, M.; Rodenberg, A.; Kopelent, R.; Probst, B.; Buchwalder, C.; Brandstätter, M.; Hamm, P.; Alberto, R. Photocatalytic H2 Production with a Rhenium/Cobalt System in Water under Acidic Conditions. *Eur. J. Inorg. Chem.* **2012**, *2012* (1), 59–64. https://doi.org/10.1002/ejic.201100883.

(20) Rodenberg, A.; Orazietti, M.; Mosberger, M.; Bachmann, C.; Probst, B.; Alberto, R.; Hamm, P. Quinones as Reversible Electron Relays in Artificial Photosynthesis. *ChemPhysChem* **2016**, *17* (9), 1321–1328. https://doi.org/10.1002/cphc.201501085.

(21) Gatty, M. G.; Pullen, S.; Sheibani, E.; Tian, H.; Ott, S.; Hammarström, L. Direct Evidence of Catalyst Reduction on Dye and Catalyst Co-Sensitized NiO Photocathodes by Mid-Infrared Transient Absorption Spectroscopy. *Chem. Sci.* **2018**, *9* (22), 4983–4991. https://doi.org/10.1039/C8SC00990B.

(22) Luong, J. C.; Nadjo, L.; Wrighton, M. S. Ground and Excited State Electron Transfer Processes Involving Fac-Tricarbonylchloro(1,10-Phenanthroline)Rhenium(I). Electrogenerated Chemiluminescence and Electron Transfer Quenching of the Lowest Excited State. *J. Am. Chem. Soc.* **1978**, *100* (18), 5790–5795. https://doi.org/10.1021/ja00486a033.

(23) Chen, P.; Duesing, R.; Graff, D. K.; Meyer, T. J. Intramolecular Electron Transfer in the Inverted Region. *J. Phys. Chem.* **1991**, *95* (15), 5850–5858. https://doi.org/10.1021/j100168a027.

(24) Katz, N. E.; Mecklenburg, S. L.; Graff, D. K.; Chen, P.; Meyer, T. J. Calculation of Electron-Transfer Rate Constants in the Inverted Region from Absorption Spectra. *J. Phys. Chem.* **1994**, *98* (36), 8959–8961. https://doi.org/10.1021/j100087a024.

(25) Whitten, D. G.; Yau, J. C. N. Photochemical Electron Transfer: Reduction of Tin Porphyrins in the Presence of Stannous Chloride. *Tetrahedron Lett.* **1969**, *10* (36), 3077–3080.

(26) Zhou, J.; Shah, R. P.; Findley, B. R.; Braun, C. L. Long Distance Photoinduced Electron Transfer in Solutions: A Mechanism for Producing Large Yields of Free Ions by Electron Transfer Quenching. *J. Phys. Chem. A* **2002**, *106* (1), 12–20. https://doi.org/10.1021/jp012808r.

(27) Dereka, B.; Koch, M.; Vauthey, E. Looking at Photoinduced Charge Transfer Processes in the IR: Answers to Several Long-Standing Questions. *Acc. Chem. Res.* **2017**, *50* (2), 426–434. https://doi.org/10.1021/acs.accounts.6b00538.

(28) Clark, C. D.; Hoffman, M. Z. Effect of Solution Medium on the Rate Constants of Excited-State Electron-Transfer Quenching Reactions of Ruthenium(II)-Diimine Photosensitizers. *Coord. Chem. Rev.* **1997**, *159*, 359–373. https://doi.org/10.1016/S0010-8545(96)01297-0.

(29) Meyer, T. J.; Meyer, G. J.; Pfennig, B. W.; Schoonover, J. R.; Timpson, C. J.; Wall, J. F.; Kobusch, C.; Chen, X.; Peek, B. M.; Wall, C. G.; et al. Molecular-Level Electron Transfer and Excited State Assemblies on Surfaces of Metal Oxides and Glass. *Inorg. Chem.* **1994**, *33* (18), 3952–3964. https://doi.org/10.1021/ic00096a020.

(30) Dattelbaum, D. M.; Omberg, K. M.; Schoonover, J. R.; Martin, R. L.; Meyer, T. J. Application of Time-Resolved Infrared Spectroscopy to Electronic Structure in Metal-to-Ligand Charge-Transfer Excited States. *Inorg. Chem.* **2002**, *41* (23), 6071–6079. https://doi.org/10.1021/ic020400i.

(31) Dattelbaum, D. M.; Meyer, T. J. Metal-to-Ligand Charge Transfer Excited-State ν(CO) Shifts in Rigid Media. *J. Phys. Chem. A* **2002**, *106* (18), 4519–4524. https://doi.org/10.1021/jp014057z.

(32) El Nahhas, A.; Cannizzo, A.; van Mourik, F.; Blanco-Rodríguez, A. M.; Záliš, S.; Vlček, A.; Chergui, M. Ultrafast Excited-State Dynamics of [Re(L)(CO) 3 (Bpy)] n Complexes: Involvement of the Solvent. *J. Phys. Chem. A* **2010**, *114* (22), 6361–6369. https://doi.org/10.1021/jp101999m.

(33) Neuthe, K.; Bittner, F.; Stiemke, F.; Ziem, B.; Du, J.; Zellner, M.; Wark, M.; Schubert, T.; Haag, R. Phosphonic Acid Anchored Ruthenium Complexes for ZnO-Based Dye-Sensitized Solar Cells. *Dye. Pigment.* **2014**, *104*, 24–33. https://doi.org/10.1016/j.dyepig.2013.12.018.

(34) Wang, Y.; Asbury, J. B.; Lian, T. Ultrafast Excited-State Dynamics of Re(CO)3Cl(Dcbpy) in Solution and on Nanocrystalline TiO2 and ZrO2 Thin Films. *J. Phys. Chem. A* **2000**, *104* (18), 4291–4299. https://doi.org/10.1021/jp9936648.

(35) Guerrero, G.; Mutin, P. H.; Vioux, A. Anchoring of Phosphonate and Phosphinate Coupling Molecules on Titania Particles. *Chem. Mater.* **2001**, *13* (11), 4367–4373. https://doi.org/10.1021/cm001253u.

(36) Bredenbeck, J.; Helbing, J.; Hamm, P. Continuous Scanning from Picoseconds to Microseconds in Time Resolved Linear and Nonlinear Spectroscopy. *Rev. Sci. Instrum.* **2004**, *75* (11), 4462–4466. https://doi.org/10.1063/1.1793891.

(37) Hamm, P.; Kaindl, R. A.; Stenger, J. Noise Suppression in Femtosecond Mid-Infrared Light Sources. *Opt. Lett.* **2000**, *25* (24), 1798. https://doi.org/10.1364/OL.25.001798.

(38) Kraack, J. P.; Hamm, P. Solvent-Controlled Morphology of Catalytic Monolayers at Solid-Liquid Interfaces. *J. Phys. Chem. C* **2018**, *122* (4), 2259–2267. https://doi.org/10.1021/acs.jpcc.7b12421.

(39) Díaz-Torres, R.; Alvarez, S. Coordinating Ability of Anions and Solvents towards Transition Metals and Lanthanides. *Dalt. Trans.* **2011**, *40* (40), 10742. https://doi.org/10.1039/c1dt11000d.

(40) El Nahhas, A.; Consani, C.; Blanco-Rodríguez, A. M.; Lancaster, K. M.; Braem, O.; Cannizzo, A.; Towrie, M.; Clark, I. P.; Záliš, S.; Chergui, M.; et al. Ultrafast Excited-State Dynamics of Rhenium(I) Photosensitizers [Re(Cl)(CO)3(N,N)] and [Re(Imidazole)(CO)3(N,N)]+: Diimine Effects. *Inorg. Chem.* **2011**, *50* (7), 2932–2943. https://doi.org/10.1021/ic102324p.

(41) Vlček, A. Ultrafast Excited-State Processes in Re(I) Carbonyl-Diimine Complexes: From Excitation to Photochemistry. In *Photophysics of Organometallics*; Lees, A., Ed.; Springer: Berlin Heidelberg, 2009; pp 115–158. https://doi.org/10.1007/3418_2009_4.

(42) Wrighton, M.; David, L. The Nature of the Lowest Excited State in Tricarbonylchloro-1,10-Phenanthrolinerhenium(I) and Related Complexes. *J. Am. Chem. Soc.* **1974**, *96* (4), 998–1003. https://doi.org/10.1021/ja00811a008.

(43) Cannizzo, A.; Blanco-Rodríguez, A. M.; El Nahhas, A.; Šebera, J.; Záliš, S.; Vlček, A.; Chergui, M. Femtosecond Fluorescence and Intersystem Crossing in Rhenium(I) Carbonyl−Bipyridine Complexes. *J. Am. Chem. Soc.* **2008**, *130* (28), 8967–8974. https://doi.org/10.1021/ja710763w.

(44) Bredenbeck, J.; Helbing, J.; Hamm, P. Labeling Vibrations by Light: Ultrafast Transient 2D-IR Spectroscopy Tracks Vibrational Modes during Photoinduced Charge Transfer. *J. Am. Chem. Soc.* **2004**, *126* (4), 990–991. https://doi.org/10.1021/ja0380190.

(45) Johnson, F. P. A.; George, M. W.; Hartl, F.; Turner, J. J. Electrocatalytic Reduction of CO2 Using the Complexes [Re(Bpy)(CO) 3 L] n (n = +1, L = P(OEt) 3 , CH 3 CN; n = 0, L = Cl - , Otf - ; Bpy = 2,2‘-Bipyridine; Otf - = CF 3 SO 3) as Catalyst Precursors: Infrared Spectroelectrochemical Investigation. *Organometallics* **1996**, *15* (15), 3374–3387. https://doi.org/10.1021/om960044+.

(46) Kowalski, J. A.; Casselman, M. D.; Kaur, A. P.; Milshtein, J. D.; Elliott, C. F.; Modekrutti, S.; Attanayake, N. H.; Zhang, N.; Parkin, S. R.; Risko, C.; et al. A Stable Two-Electron-Donating Phenothiazine for Application in Nonaqueous Redox Flow Batteries. *J. Mater. Chem. A* **2017**, *5* (46), 24371–24379. https://doi.org/10.1039/C7TA05883G.

(47) Hayen, H.; Karst, U. Analysis of Phenothiazine and Its Derivatives Using LC/Electrochemistry/MS and LC/Electrochemistry/Fluorescence. *Anal. Chem.* **2003**, *75* (18), 4833–4840. https://doi.org/10.1021/ac0346050.

(48) Olmsted, J.; Meyer, T. J. Factors Affecting Cage Escape Yields Following Electron-Transfer Quenching. *J. Phys. Chem.* **1987**, *91* (6), 1649–1655. https://doi.org/10.1021/j100290a071.

(49) Van Stokkum, I. H. M.; Larsen, D. S.; Van Grondelle, R. Global and Target Analysis of Time-Resolved Spectra. *Biochim. Biophys. Acta - Bioenerg.* **2004**, *1657* (2–3), 82–104. https://doi.org/10.1016/j.bbabio.2004.04.011.

(50) Worl, L. A.; Duesing, R.; Chen, P.; Ciana, L. Della; Meyer, T. J. Photophysical Properties of Polypyridyl Carbonyl Complexes of Rhenium(I). *J. Chem. Soc. Dalt. Trans.* **1991**, No. S, 849–858. https://doi.org/10.1039/DT9910000849.

(51) Yi, X.; Zhao, J.; Wu, W.; Huang, D.; Ji, S.; Sun, J. Rhenium(i) Tricarbonyl Polypyridine Complexes Showing Strong Absorption of Visible Light and Long-Lived Triplet Excited States as a Triplet Photosensitizer for Triplet–Triplet Annihilation Upconversion. *Dalt. Trans.* **2012**, *41* (29), 8931. https://doi.org/10.1039/c2dt30804e.

(52) Georgopoulos, M.; Hoffman, M. Z. Cage Escape Yields in the Quenching of Tris (2,2’-Bipyridine)Ruthenium(II) by Methylviologen: Presence of Triethanolamine as a Sacrificial Electron Donor. *J. Phys. Chem.* **1991**, *95* (20), 7717–7721. https://doi.org/10.1021/j100173a031.

(53) Chen, P.; Duesing, R.; Tapolsky, G.; Meyer, T. J. Intramolecular Electron Transfer in the Inverted Region. *J. Am. Chem. Soc.* **1989**, *111* (21), 8305–8306. https://doi.org/10.1021/ja00203a056.

(54) Christ, C. S.; Yu, J.; Zhao, X.; Palmore, G. T. R.; Wrighton, M. S. Intermolecular and Intramolecular Excited-State Electron Transfer Involving Electrode-Confined Rhenium Carbonyl Complexes: Toward Molecule-Based Systems for Light Absorption, Charge Separation, and Optical Energy Conversion. *Inorg. Chem.* **1992**, *31* (22), 4439–4440.

https://doi.org/10.1021/ic00048a003.

(55) Berg, O. G.; von Hippel, P. H. Diffusion-Controlled Macromolecular Interactions. *Annu. Rev. Biophys. Biophys. Chem.* **1985**, *14* (1), 131–158. https://doi.org/10.1146/annurev.bb.14.060185.001023.

(56) Ge, A.; Rudshteyn, B.; Psciuk, B. T.; Xiao, D.; Song, J.; Anfuso, C. L.; Ricks, A. M.; Batista, V. S.; Lian, T. Surface-Induced Anisotropic Binding of a Rhenium CO2-Reduction Catalyst on Rutile TiO2(110) Surfaces. *J. Phys. Chem. C* **2016**, *120* (37), 20970–20977. https://doi.org/10.1021/acs.jpcc.6b03165.

(57) Anfuso, C. L.; Snoeberger, R. C.; Ricks, A. M.; Liu, W.; Xiao, D.; Batista, V. S.; Lian, T. Covalent Attachment of a Rhenium Bipyridyl CO2 Reduction Catalyst to Rutile TiO2. *J. Am. Chem. Soc.* **2011**, *133* (18), 6922–6925. https://doi.org/10.1021/ja2013664.

(58) Hu, K.; Meyer, G. J. Lateral Intermolecular Self-Exchange Reactions for Hole and Energy Transport on Mesoporous Metal Oxide Thin Films. *Langmuir* **2015**, *31* (41), 11164–11178. https://doi.org/10.1021/acs.langmuir.5b02129.

(59) Ardo, S.; Meyer, G. J. Characterization of Photoinduced Self-Exchange Reactions at Molecule–Semiconductor Interfaces by Transient Polarization Spectroscopy: Lateral Intermolecular Energy and Hole Transfer across Sensitized TiO 2 Thin Films. *J. Am. Chem. Soc.* **2011**, *133* (39), 15384–15396. https://doi.org/10.1021/ja200652r.

Figure for TOC